ORIENTAL JOURNAL OF CHEMISTRY
An International Open Access, Peer Reviewed Research Journal
www.orientjchem.org
ISSN: 0970-020 X
CODEN: OJCHEG
2024, Vol. 40, No.(3):
Pg. 758-766

Biosynthesis of Copper oxide Nanoparticles Using *Azadirachta indica* Seed Extract and Its Characterization

P. KALAIVANI[1] and G. MATHUBALA[2*]

[1]Research Scholar, Department of Chemistry, Bharath Institute of Higher Education and Research, BIST, Chennai-73, India.
[2*]Professor and Head, Department of Chemistry, Bharath Institute of Higher Education and Research, BIST, Chennai-73, India.
*Corresponding author E-mail: kalaivanipolur94@gmail.com; madhu2705@gmail.com

http://dx.doi.org/10.13005/ojc/400317

(Received: February 27, 2024; Accepted: May 06, 2024)

ABSTRACT

In the current era, green synthesis stands out as the optimal approach for nanoparticle production, owing to its myriad advantages over traditional methods. Copper oxide nanoparticles (CuONP) using botanical extracts possess distinctive attributes ascribed to the phytochemicals of the extracts. These extracts can increase and maintain stability and modify the dimensions and morphology of CuONP. This green synthesis process is notable for its environmental compatibility, economic efficiency, and broad applicability, particularly in catalysis and biomedical domains. The present investigation explores synthesizing CuONP using the extract from *Azadirachta indica (A. indica)* seeds as a stabilizing and reducing agent. The CuONP prepared was characterized using X-ray diffraction, which revealed a mean particle size between 35 nm. Fourier Transform Infrared spectroscopy confirmed the presence of copper oxide evidenced by the stretching absorptional vibrations of functional groups. High-Resolution Transmission Electron Microscopy (HRTEM) and Scanning Electron Microscopy evaluated the nanoparticles' morphology. The findings significantly contribute to the expanding knowledge base on eco-friendly approaches to nanoparticle synthesis, emphasizing the diverse potential applications of CuONP synthesized through this environmentally conscious method.

Keywords: Copper Sulfate, CuO Nanoparticles, *Azadirachta indica*, Green Synthesis.

INTRODUCTION

Nanostructured metal oxides have garnered considerable attention across various scientific fields, spanning materials chemistry, medicine, biomedical engineering, electronics, environmental science, energy research, sensor technology, and information technology. Unlike noble metals like gold, silver, and platinum, metal oxides incorporate oxygen during the formation of their crystalline nanoparticles, requiring high-temperature methods such as annealing or calcination, often exceeding 300°C[1]. Nanoparticles (NPs) are essential in cancer therapy because of their distinctive attributes: form, size, dispersion, and surface-to-volume ratio. In Inorganic metal NPs like silver, gold, and cobalt are commonly

employed because of their unique characteristics. These NPs serve dual purposes: facilitating drug delivery and acting as therapeutic agents, making them essential components of anticancer treatment, including geometries, redox states, and reactivity, which remain inaccessible to organic compounds[2]. Ecological approaches for generating metal or metal oxide NPs in volve reducing metal complexes in diluted solutions to form colloidal dispersions of metals. This strategy is predicated on using particular compounds capable of reducing metal precursors to NPs; natural substances, including microbial and plant extracts, have garnered considerable attention Furthermore, these extracts stabilize the resulting NPs and serve as insitu capping and reducing agents. They aid in reducing metal ions from a positively oxidized state to a zero electrostatic potential. Consequently, the aggregation of nanoparticles caused by chemical and physical interactions is prevented. The appearance of inherent compounds within the extract substantially impacts the characteristics and distribution of particle size[3]. Augmenting the ratio of reductants to reactants within the extract enhances the reaction pace, producing nanoparticles with reduced dimensions. Different plant extracts have been used to synthesize metal oxide nanoparticles due to escalating consumer needs. Calcium oxide (CaO), classified as an alkaline earth metal oxide, finds application across diverse sectors, including varistors, solar cells, cosmetics, and catalysts. In their study, Dani *et al.,* (2016) investigated the environmentally friendly synthesis of sucrose-coated S-CaO-NPs, utilizing an aqueous extract derived from *A. Indica* leaves in conjunction with calcium nitrate, sodium hydroxide, and sucrose. Their research also explored the antimicrobial properties of both coated S-CaO-NPs and uncoated CaO-NPs, revealing that sucrose-coated CaO-NPs demonstrated larger zones of inhibition against bacillus bacteria[4]. Furthermore, the researchers developed chemical sensors capable of detecting 2-butanone, employing a glassy carbon electrode (GCE) that underwent modification with Mn_3O_4-NPs. The sustainable production of these Mn_3O_4-NPs enhances the GCE surface's capacity to attract oxygen molecules, thereby increasing the number of active sites. Bhuyan *et al.,* (2015) employed the co-precipitation technique involving *A. Indica* leaves for zinc oxide NPs. Subsequently, these NPs were characterized using XRD, FT-IR spectroscopy, UV-Visible spectroscopy, and TEM5. Green synthesis methods have been utilized to fabricate Co_3O_4 NPs, employing various approaches such as HPCM, glycine, cobalt(II) nitrate, and Al leaf extract. X-ray diffraction (XRD) and high-resolution transmission electron microscopy confirmed the NPs polycrystalline structure. Cr_5O_{12} shell NPs were synthesized by employing *A. Indica* leaf extract and potassium dichromate as a chromium source[6]. Examination of the FTIR spectrum indicated the presence of flavonoids, polyphenols, and terpenoids with carboxyl groups, hinting at potential capping agent functionalities. Fe_3O_4@ZnO core-shell NPs were also fabricated through hydrothermal and phytotechniques[7]. Researchers commonly prefer Copper (Cu) to other metals for preparing NPs, as it is economical and has effective stability. Copper can regulate surface charge and initiate oxidative stress within cells due to its distinctive electronic configuration and co-factor function in enzyme redox cycling[8]. In transition metals, copper actively engages in diverse biological roles, such as catalytic activity, electron transfer, and structural modification. Its efficacy in eliminating cancer cells primarily stems from its ability to induce oxidative stress[9]. Copper's role in cancer therapy is due to its multifaceted attributes, including cost-effectiveness, stability, and its profound impact on biological functions, particularly in instigating oxidative stress to eliminate cancer cells[10]. Plant-derived copper nanoparticles (CuNP) are recognized for their cost-effectiveness and safety; *A.indica* is a medicinal plant that has been used for a long time and is commonly found in tropical and semi-tropical locations. It distinguishes itself from other plant sources by its wide range of medical applications. The leaves, flowers, fruits, and seeds of this plant exhibit encouraging chemopreventive and therapeutic attributes, making it an apt choice for medicinal, surgical, and pharmaceutical drugs[11,12], and extracts from this plant demonstrate selective cytotoxicity towards cancer cells, minimizing toxicity during cancer therapy. *A. Indica* botanical products impede the growth and proliferation of cancerous cells by disrupting the progression of the cell cycle. Furthermore, scientific research has shown that *A. Indica* seed oil inhibits the proliferation and multiplication of Hela cervical cancer cells[13]. Despite significant advancements in utilizing *A. Indica* extracts for treating cancer, the precise mechanism responsible for their anticancer effects remains unclear. Prior research has demonstrated that certain constituents of *A. Indica* impedes

NF-κB signaling pathways, enhances the susceptibility of cancer cells to radiotherapy and immunotherapy, triggers apoptosis and tumor-specific antiproliferative effects, and exhibits significantly lower toxicity towards healthy cells[14]. Literature on CuONP synthesis by *A. indica* lacks in-depth characterization based on early studies on different metals. Specifically, detailed analysis of its physicochemical properties, stability, and application potentials is scarce and is crucial for exploring its diverse applications in medicine, agriculture, and environmental remediation. Hence, there is a pressing need for comprehensive studies focusing on synthesis, process optimization and thorough characterization using advanced techniques like TEM, XRD, and FTIR, alongside exploring its potential applications to bridge this gap in the literature and harness its full potential. The current research employs *A. indica* seeds extract as a reducing agent NPs prepare CuONP Various evaluation methods, including XRD, TEM, SEM, and UV, were used to characterize the nanoparticles for validation.

MATERIALS AND METHODS

Collecting Plant Seeds

The *A. indica* plant's seed was obtained from a Polur, Tiruvannamalai District garden, Tamil Nadu, India. Subsequently, it was thoroughly washed with distilled water, adhering to professional standards. The moisture was completely removed, the seed was cleaned and dried under a sunshade, and then powdered by mechanical grinding[15].

Fig.1. *A. indica* Plant Seeds

Preparation of Plant Seed Extract

The surface moisture of the seed was first eliminated by drying it in the air under a sunshade. Using 200 mL of double-distilled water, 10 g of powdered *A. indica* seeds were heated at 50°C for 30 min while stirring continuously for 2 hours. The suspension was allowed to stand undisturbed until it reached room temperature. The extract was clarified by passing it through Whatman No. 1 filter paper to achieve a clear solution. The filtered aqueous solution was refrigerated at 4°C for further use 16.

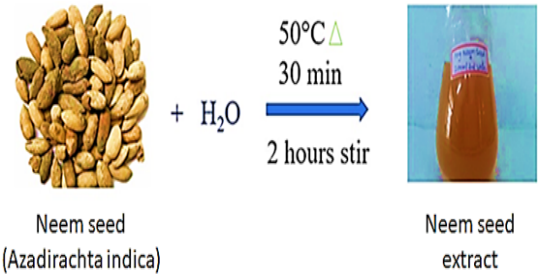

Fig. 2. The preparation of *A. indica* seeds extract

Synthesis of CuONP

A solution containing 1 mM copper sulfate ($CuSO_4.5H_2O$) with water and stirred with 100 mL of seed extract for 5 h at 75°C. After incubating for 24 h at 60°C, the mixture's color changed from blue to deep brown, suggesting the potential formation of CuONPs and a decrease in Cu^{2+} ions. CuONPs was subsequently obtained by subjecting the product to a rigorous cleansing process utilizing deionized water and ethanol, followed by a drying period of 10 h at 60°C[17].

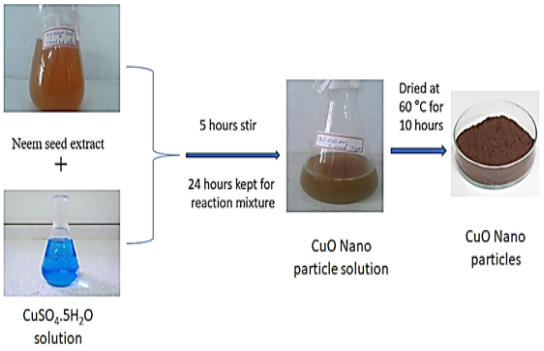

Fig. 3. Diagram demonstrating the creation of CuONPs

The neem extract contains compounds capable of reducing copper ions from a higher oxidation state (Cu^{2+}) to a lower oxidation state (Cu^0). This reduction reaction can be represented as follows:

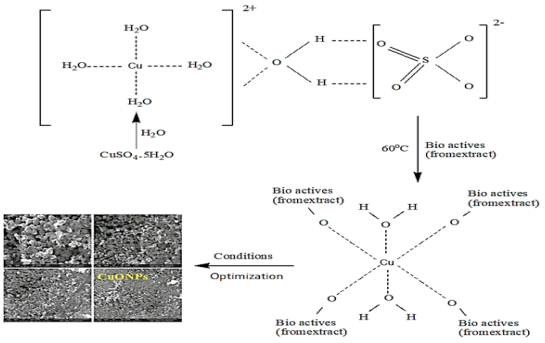

This redox reaction involves the transfer of electrons from the reducing agents present in the *A. indica* extract to the copper ions in the solution, forming a complex involving multiple copper ions. Once the copper ions are reduced to a lower oxidation state, they can further react to form CuONPs. This can occur through various mechanisms, including atmospheric oxygen oxidation of copper (I) ions. In this reaction, copper ions (Cu^0) react with oxygen (O_2) to form copper oxide (2CuO), which is a reddish-brown solid. Further reaction and growth of these NPs can occur depending on the concentration of copper ions and the reaction conditions. *A. indica* extract acts as a reducing agent in converting copper sulfate solution to CuONPs. It facilitates the reduction of copper ions to lower oxidation states, which then undergo further reactions to form copper oxide nanoparticles.

$2Cu+O_2 \rightarrow 2CuO$

X-ray Diffraction Analysis

XRD analysis confirmed the crystalline structure of the produced CuONPs. Before XRD analysis, the centrifuged and dried sample was placed on a small glass slide and exposed to vacuum drying at 45°C overnight. Following the vacuum-drying process, the CuONPs was examined for XRD analysis. A powder X-ray diffraction analysis was conducted utilizing an analytical XPERT PRO diffractometer functioning at 45 kV and 30 mA, employing CuKα radiation (λ=1.542). The diffraction patterns exhibited a wavelength variation of 10–60° 2θ. The intensities of the diffracted X-rays were recorded throughout the procedure[18,19].

Scanning Electron Microscope

SEM (JEOL JSM 5600) studies were conducted to examine the CuONP surface properties. The powder underwent a series of steps, including washing it with distilled water and dehydration using a graded ethanol solution up to 100%. The specimen was later placed on a copper grid coated with carbon and then analyzed using SEM at an acceleration voltage of 80 kilovolts (kV)[20].

High-Resolution Transmission Electron Microscopy

The HR-TEM studies examined the morphological and topographical characteristics of the CuONPs. A thin film comprising these nanoparticles was coated on a carbon-coated copper grid with a 30×30 µm pore size, and any surplus solution was subsequently eliminated using absorbent paper. The grid was subsequently dried for five minutes under a mercury lamp. The Tecnai G2 Spirit Biotwin instrument was utilized to obtain micrographs at an estimated accelerating voltage of 80 kV[21].

FT-IR Spectroscopy

The spectrum data were acquired using a Shimadzu 8400S Fourier transform infrared spectrophotometer (FTIR) coupled with a diffuse reflectance accessory, and the measurements were conducted within the 4000 to 400 cm^{-1} interval. At a 1:100 (w/w) weight ratio, the dehydrated inorganic metal nanoparticles were mixed with the alkali halide potassium bromide (KBr) and subjected to a rigorous pulverization process utilizing a mortar and pestle. Subsequently, the mixtures were compressed into pellets using a pellet press equipped with dual pistons housed in a cylindrical chamber. The pressures applied to the press reached a maximum of 25,000 psi, and the pellets were held in place for variable durations in a vacuum environment. After the pistons were de-engaged following compression, the resulting translucent pellets were introduced into the receptacle of the spectrophotometer. A spectrum was acquired to examine the functional groups in the sample since potassium bromide does not absorb infrared light between 4000 and 400 cm^{-1} [22].

UV-spectroscopy

CuONPs was analyzed for UV absorption spectrum, utilizing a Hitachi 330 spectrophotometer. Plasmon peaks signal the presence of different nanoparticles detected in the 200–900 nm spectral range. Deionized water was utilized as the reference solution throughout the analysis, providing a baseline for comparison[23].

RESULTS AND DISCUSSION

Structural properties of CuONPs

Figure 4 depicts the XRD pattern of CuONPs, which was synthesized using seed extract from *A. indica*. In the accompanying table (Table 1), the intensity and location of the peaks are specified in detail. Comparison with the JCPDS data (77-1898) indicates good agreement with the reported values for a monoclinic structure[24]. Three prominent peak values at 2θ angles of 20.9°, 28.5°, and 56.3° are observed within the 20° to 90° range, corresponding

to crystallographic planes (hkl) 212, 204, and 262 from the JCPDS database[25]. The CuONPs demonstrated a range in average particle size from 35 nm, confirming that they were CuONPs derived from plant extract[26]. The average particle diameter (PD) for various specimens was determined from the main peak using the Debye-Scherrer equation, which relates peak width broadening to particle size[27].

$$PD = 0.89\ \lambda / \beta\cos\theta$$

Table 1: The dimensions of the CuONP particle

θ2 of the intense Peak (deg)	θ of the intense peak (deg)	FWHM of intense peak (β)	Size of the particle (D) nm	d spacing	Plane (hkl)
25.7	12.8	0.2323	35	3.457	123

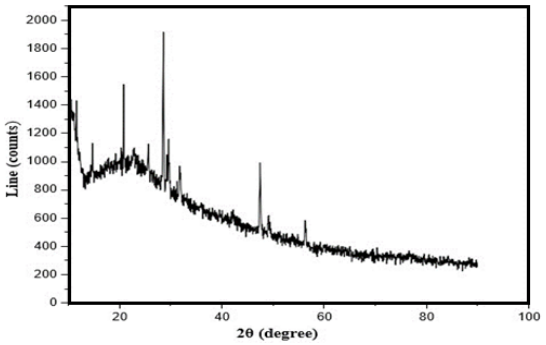

Fig. 4. XRD pattern of Synthesis of CuONP from *A. indica* Seed extract

Morphological analysis

Scanning Electron Microscopy

The morphology of CuONPs was analyzed using a SEM. As shown in Fig. 5, the images revealed agglomerated structures resembling spheres for the synthesized CuONP[28,29], aligning with previously reported studies for their shape and uniformity. These agglomerated nanosized particles, indicated the synthesis of CuONPs with distinct morphological features, as illustrated in the micrographs captured in Figure 5[30].

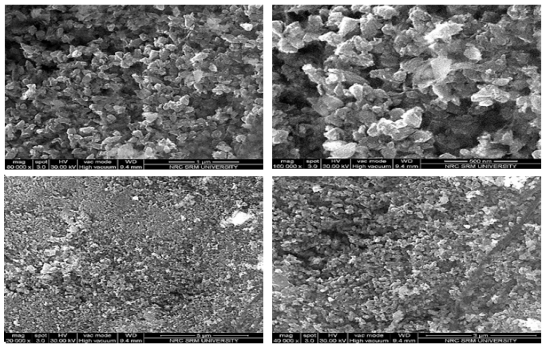

Fig. 5. SEM image of Synthesized CuONP from *A. indica* seed extract

HR-TEM

The CuONPs morphology and particle size, synthesized, were visualized through HR-TEM. This imaging technique provided detailed insight into the morphology and shape of the CuONP. In Fig. 6, the HR-TEM image displays the synthesized CuONPs, revealing various morphologies (A, B, C, D) indicative of nanoparticle aggregation and a sphere-like nanostructure. These morphologies aligned well with the observations from SEM in our study[31,32]. The particles exhibited quasi-spherical shapes and were uniformly sized, with diameters spanning from 1 to 20 nanometers.

Furthermore, the verification of the singular crystalline composition of the CuONPs was accomplished by the presence of clearly defined circular patches in the selected area of electron diffraction[33] (Fig. 6 (D)). HR-TEM analysis data revealed that most NPs exhibited distinct segregation, with consistent spacing between them. It is worth mentioning that the diameter of CuONPs, as determined by TEM analysis, differed significantly from that acquired by SEM, attributed to disparities in sample preparation techniques, with CuONP appearing more dehydrated in TEM compared to the hydrated state observed in SEM experiments.

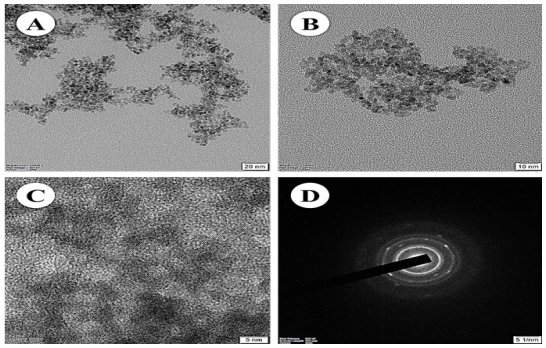

Fig. 6. HR-TEM image of Synthesized CuONP from *A. indica* seed extract

FT-IR absorption (Functional groups analysis)

The FTIR absorption spectra of vacuum-dried CuONPs, synthesized via biosynthesis,

are illustrated in Fig. 7. Peaks are observed within these spectra around 3253 cm^{-1} and 2948 cm^{-1}, corresponding to elongation vibrations in primary and secondary amines. A peak between 1240 cm^{-1} and 1250 cm^{-1} indicates C-O vibration, which is consistent with the peak observed in the seed extract and suggests that there were only minor modifications during the formation of the nanoparticles. Similarly, a prominent peak observed between 1630 cm^{-1} and 1650 cm^{-1} indicates the presence of C=C vibration, which signifies a consistent feature mimicking the equivalent mode found in the seed extract. It suggests the possibility of changes occurring in the carbon-carbon double bond during the production of nanoparticles. The absorption peak detected between 2940 cm^{-1} and 2930 cm^{-1} is associated with the vibration of CH bonds. This closely resembles the vibration mode, indicating minimal changes in the hydrocarbon chain during nanoparticle formation. The peak within the 3390 cm^{-1} to 3480 cm^{-1} range reflects O-H vibration suggesting modifications or interactions affecting the hydroxyl group. The aldehyde peak at 2356 cm-1 is associated with the frequency of CH bonds. The absorption peaks at 1439, 1538, and 1651 cm^{-1} indicates the existence of CC groups from aromatic rings and phenols and, correspondingly, the stretching vibration of conjugated carbonyl (–C=O) molecules. These traits point to pteridophyte cells, which the plant extract mostly contains[34,35]. It is believed that the carbonyl group (C=O) reacting with the nanoparticles is responsible for the change in the 1600 cm^{-1}. FTIR peaks between 1240 cm^{-1} and 1280 cm^{-1} indicates the presence of amide III band, characteristic of the random coil structure found in proteins. Previous research on CuONPs synthesis has also identified a band at 1076 cm^{-1}, which is associated with the bending vibrations in the amides II band.

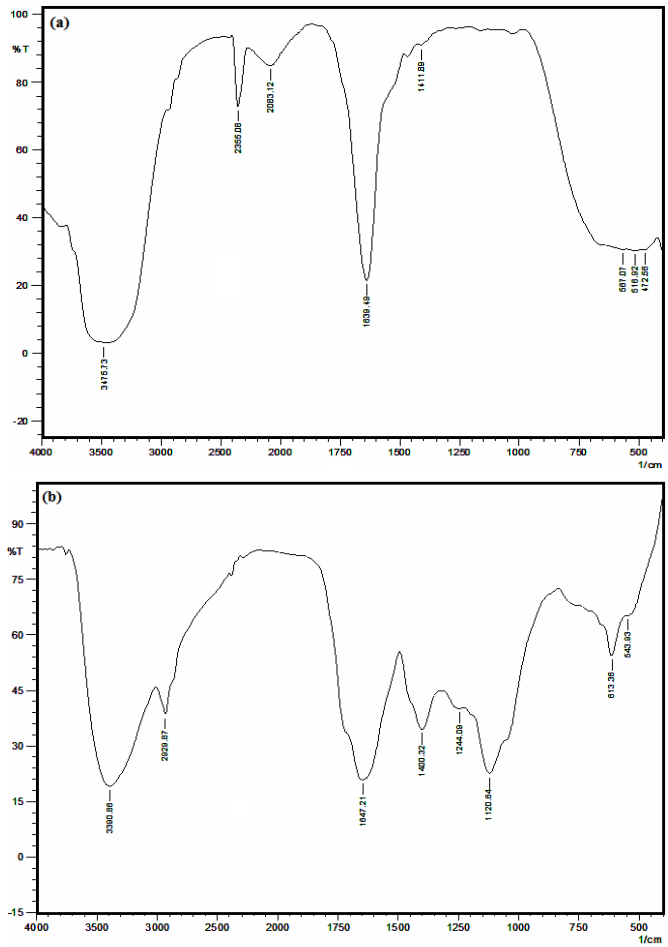

Fig. 7. FT-IR spectrum of (a) *A. indica* seed extract (b) Synthesized CuONP from *A. indica* seed extract

The investigation and presentation of the FT-IR spectrum wavelength range of 500 cm^{-1} to 4000 cm^{-1} is depicted in Fig. 7, and the respective vibration frequency of *A. Indica* Seed extract and CuONPs are listed in Table 2.

Table 2: Types of vibrations of *A. Indica* Seed extract of CuONP

Types of vibrations	*A. indica* Seeds extract (cm^{-1})	CuONP (cm^{-1})
ν(Cu-O)	_	613
ν(C-O)	1240	1244
ν(C=C)	1639	1647
ν(C-H)	2935	2929
ν(O-H)	3475	3390

UV-Spectral studies

The UV-Spectra of *A. Indica* Seed extract was obtained with de-ionized water as the solvent. The formation of CuONPs was initially verified through UV-Absorption spectroscopy, as illustrated in Fig. 8 (a,b). The brown hue or colour in the reaction mixture resulted from stimulating surface plasmon oscillations within the copper oxide particles. This color change indicates the formation of CuONPs. An investigation was carried out to examine the reduction of copper sulfate using spectrum analysis, assisted by a UV-Spectrophotometer. The peak absorption at wavelengths 235, 239, 360, 364, and 392 nm was obtained due to a π-π^* electronic transition[36,37]. The significant absorption peak detected between 401 and 409 nm in CuONPs resulted from the n-π^* electronic transition. The peak at 565 nm, along with a bathochromic shift, confirms the nanoparticle formation[38,39]. Furthermore, the molecular vibrational absorption results validate the Surface Plasmon Resonance feature inherent to CuONP[40].

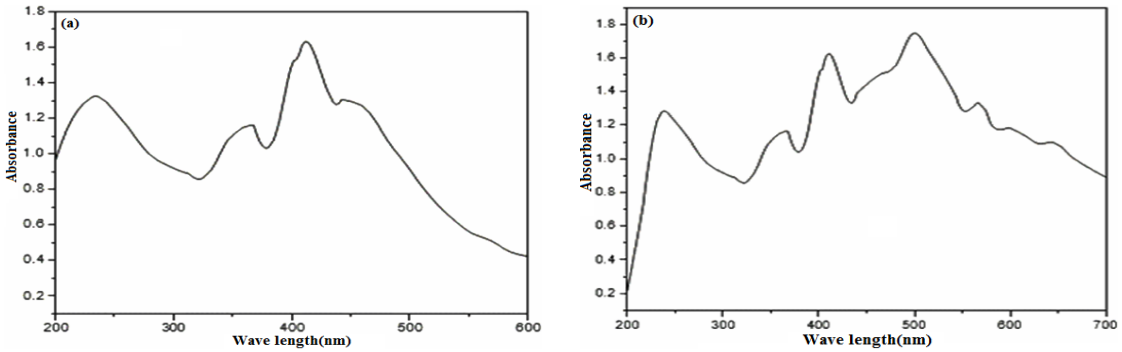

Fig. 8. UV-Spectra of (a) *A. indica* seed extract and (b) Synthesized CuONP from *A. indica* seed extract

Particle size distribution and surface characteristics of CuONPs are crucial for understanding its potential uses. HR-TEM analysis revealed the atomic composition of copper and oxygen, suggesting that a considerable portion of the nanoparticle sample, generated through thermal plasma technology, comprised copper oxide. Moreover, HR-TEM allowed direct observation of changes in the nanoparticle's morphology[41]. The presence of CuONPs was verified by color changes and by conducting analyses using UV, SEM, TEM, and XRD techniques, with findings consistent with prior research. Under typical conditions, the plant extract formed CuONPs, mirrored earlier observations in biological NPs synthesis studies[42,43]. The XRD analysis validated the crystalline structure of CuONPs, which is consistent with results documented in prior scholarly works[44]. FT-IR analyses confirmed the presence of unique absorption peaks related to the nanoparticle structure. Earlier studies suggested that certain absorption peaks of CuONPs were between 550 cm^{-1} and 600 cm^{-1}. As evident from Fig. 7, the dominant peak at 613 cm^{-1} indicates Cu-O bond elongation[45,46].

CONCLUSION

In summary, this research investigated CuONPs, analysing its elemental composition, size distribution, shape, and structure. The study employed sophisticated techniques such as TEM, UV-Vis spectroscopy, XRD, SEM, and FT-IR techniques to validate the synthesis of CuONPs in the presence of *A. indica* seed extract. This economical and environmentally friendly approach offers a simpler method for synthesizing CuONPs, with results corroborating previous studies and offering valuable insights into their potential uses. This characterization enriches our comprehension of the synthesized NPs, facilitating their informed application across various fields.

ACKNOWLEDGMENT

There was no dedicated funding from public, commercial, or non-profit organizations for this research.

Conflict of interest

Conflict of interest declared none.

REFERENCES

1. Korotcenkov, G.; Cho, B. K., *Prog. Cryst. Growth Charact. Mater.*, **2012**, *58*(4), 167–208.
2. Alshameri, A.W.; Owais, M., *OpenNano.,* **2022**, *8*, 100077.
3. Tripathy, A.; Raichur, A. M.; Chandrasekaran, N.; Prathna, T. C.; Mukherjee, A., *J. Nanoparticle Res.*, **2009**, *12*(1), 237–246.
4. Jagadeesh, D.; Prashantha, K.; Shabadi, R., *Inorg. Nano-Metal Chem.*, **2016**, *47*(5), 708–712.
5. Bhuyan, T.; Mishra, K.; Khanuja, M.; Prasad, R.; Varma, A., *Mater. Sci. Semicond. Process.*, **2015**, *32*, 55–61.
6. Patil, S. P.; Chaudhari, R. Y.; Nemade, M. S., *Talanta Open.*, **2022**, *5*, 100083.
7. Madhubala, V.; Kalaivani, T., *Appl. Surf. Sci.*, **2018**, *449*, 584–590.
8. Arif, H.; Sohail, A.; Farhan, M.; Rehman, A. A.; Ahmad, A.; Hadi, S. M., *Int. J. Biol. Macromol.*, **2018**, *106*, 569- 578.
9. Kanti Das, T.; Wati, M. R.; Fatima-Shad, K., *Arch. Neurosci.*, **2015**, *2*(2).
10. Lelievre, P.; Sancey, L.; Coll, J. L.; Deniaud, A.; Busser, B., *Cancers (Basel).,* **2020**, *12*, 3594.
11. Kasana, R. C.; Panwar, N. R.; Kaul, R. K.; Kumar, P., *Environ. Chem. Lett.*, **2017**, *15*, 233-240.
12. Alzohairy, M. A., *Evid. Based. Complement. Alternat. Med.*, **2016**, *2016*, 7382506.
13. John, A.; Raza, H., *Antioxidants (Basel, Switzerland).,* **2023**, *12*(11), 2001.
14. Dey, A.; Manna, S.; Chattopadhyay, S.; Mondal, D.; Chattopadhyay, D.; Raj, A.; Das, S.; Bag, B. G.; Roy, S., *J. Saudi Chem. Soc.,* **2019**, *23*, 222-238.
15. Amjad, R.; Mubeen, B.; Ali, S. S.; Imam, S. S.; Alshehri, S.; Ghoneim, M. M.; Alzarea, S. I.; Rasool, R.; Ullah, I.; Nadeem, M. S.; Kazmi, I., *Polymers (Basel).,* **2021**, *13*, 4364.
16. Radhakrishnan, R.; Khan, F. A.; Muthu, A.; Manokaran, A.; Savarenathan, J. S.; Kasinathan, K., *Lett. Appl. NanoBioScience.,* **2021**, *10*, 2706–2714.
17. Ananth, A.; Dharaneedharan, S.; Heo, M.-S.; Mok, Y. S., *Chem. Eng. J.*, **2015**, *262*, 179-188.
18. Dlamini, N. G., Basson, A. K., & Pullabhotla, V. S. R., *Applied Nano.*, **2023**, *4*(1), 1-24.
19. Nagar, N.; Devra, V., *Mater. Chem. Phys.*, **2018**, *213*, 44-51.
20. Tegenaw, A.; Sorial, G. A.; Sahle-Demessie, E.; Han, C., *Environ. Res.*, **2020**, *187*, 109700.
21. Mukhopadhyay, R.; Kazi, J.; Debnath, M. C., *Biomed. & amp; Pharmacother.*, **2018**, *97*, 1373-1385.
22. Sarkar, J.; Chakraborty, N.; Chatterjee, A.; Bhattacharjee, A.; Dasgupta, D.; Acharya, K., *Nanomater. (Basel, Switzerland).,* **2020**, *10*(2), 312.
23. Gondal, M. A.; Qahtan, T. F.; Dastageer, M. A.; Maganda, Y. W.; Anjum, D. H., *J. Nanosci. Nanotechnol.,* **2013**, *13*, 5759-5766.
24. Andualem, W. W.; Sabir, F. K.; Mohammed, E. T.; Belay, H. H.; Gonfa, B. A. J. Nanotechnol., 2020, 2020, 1.
25. Ijaz, F.; Shahid, S.; Khan, S. A.; Ahmad, W.; Zaman, S., *Trop. J. Pharm. Res.*, **2017**, *16*, 743-753.
26. Akintelu, S. A.; Folorunso, A. S.; Folorunso, F. A.; Oyebamiji, A. K., *Heliyon.*, **2020**, *6*(7), e04508.
27. Acharyulu, N. P. S.; Kiran, P. M.; Kollu, P.; Kalyani, R. L.; Pammi, S. V. N., *J. Bionanoscience.*, **2014**, **2014**, *3*(4), 143-149.
28. Chandra, S.; Kumar, A.; Tomar, P. K., *J. Saudi Chem. Soc.*, **2014**, *18*, 149-153.
29. Dong, C.; Cai, H.; Zhang, X.; Cao, C., *Phys. E Low-dimensional Syst. Nanostructures.,* **2014**, *57*, 12–20.
30. Veisi, H.; Karmakar, B.; Tamoradi, T.; Hemmati, S.; Hekmati, M.; Hamelian, M., *Sci. Rep.,* **2021**, *11*(1), 1983.
31. Waris, A.; Din, M.; Ali, A.; Ali, M.; Afridi, S.; Baset, A.; Ullah Khan, A., *Inorg. Chem. Commun.*, **2021**, *123*, 108369.
32. Chen, H.; Zheng, X.; Chen, Y.; Li, M.; Liu, K.; Li, X., *PLoS One.*, **2014**, *9*(3), e92871.
33. Varshney, R.; Bhadauria, S.; Gaur, M. S.; Pasricha, R., *JOM.*, **2010**, *62*(12), 102–104.

34. Mathews, R. P.; Singh, B. D.; Singh, H.; Singh, V. P.; Singh, A., *J. Geol. Soc. India*., **2018**, *91* (3), 281–289.
35. Baskaran, X.; Geo Vigila, A. V.; Parimelazhagan, T.; Muralidhara-Rao, D.; Zhang, S., *Int. J. Nanomedicine*., **2016**, *11*, 5789–5806.
36. Rafique, M.; Shaikh, A. J.; Rasheed, R.; Tahir, M. B. Gillani, S. S. A.; Usman, A.; Imran, M.; Zakir, A.; Khan, Z. U. H.; Rabbani, F., *J. Inorg. Organomet. Polym. Mater*., **2018**, *28*(6), 2455–2462.
37. Zhang, G.; Savateev, A.; Zhao, Y.; Li, L.; Antonietti, M. *J. Mater. Chem. A*., **2017**, *5*(25), 12723–12728.
38. Gaber, M.; El-Sayed, Y. S.; El-Baradie, K.; Fahmy, R. M., *J. Mol. Struct*., **2013**, *1032*, 185–194.
39. Gebremedhn, K.; Kahsay, M. H.; Aklilu, M. *J. Pharm. Pharmacol*., **2019**, *7*(6).
40. Saloki, A.; Daharwal, S. J., *Asian J. Pharm. Clin. Res*., **2023**, 172-176.
41. Marino, E.; Huijser, T.; Creyghton, Y.; van der Heijden, A., *Surf. Coatings Technol.,* **2007**, *201*(22–23), 9205–9208.
42. Ahmad, H.; Venugopal, K.; Bhat, A. H.; Kavitha, K.; Ramanan, A.; Rajagopal, K.; Srinivasan, R.; Manikandan, E., *Pharm. Res*., **2020**, *37*(12).
43. Sadiq, M. U.; Shah, A.; Haleem, A.; Shah, S. M.; Shah, I., *Nanomaterials*., **2023**, *13*(13), 2019.
44. Vaseem, M.; Lee, K. M.; Kim, D.Y.; Hahn, Y.-B., *Mater. Chem. Phys*., **2011**, *125*(3), 334–341.
45. Hasheminya, S.-M.; Dehghannya, *J. Part. Sci. Technol*., **2019**, *38*(8), 1019–1026.
46. Sagadevan, S.; Vennila, S.; Marlinda, A. R.; Al-Douri, Y.; Rafie Johan, M.; Anita Lett., *J. Appl. Phys. A*., **2019**, *125*(8).